Available online at www.sciencedirect.com
SCIENCE DIRECT
Journal of Molecular Catalysis A: Chemical 251 (2006) 255–262
JOURNAL OF MOLECULAR CATALYSIS A: CHEMICAL
www.elsevier.com/locate/molcata

Ionic-strength dependence of electron-transfer reactions of Keggin heteropolytungstates: Mechanistic probes of O_2 activation in water

Yurii V. Geletii [a], Ira A. Weinstock [b,*]

[a] *Department of Chemistry, City College of New York, New York, NY 10031, USA*
[b] *Department of Chemistry, Emory University, Atlanta, GA 30322, USA*

Available online 7 March 2006

Abstract

Kinetic data needed to use α-$AlW_{12}O_{40}^{6-}$ (α-$\mathbf{2}_{1e}$) as well-defined probe for investigating electron-transfer processes in water is evaluated using the extended Debye–Hückel equation. First, rate constants, as a function of ionic strength in water, are determined for electron self-exchange reactions between a series of $AlW_{12}O_{40}^{n-}$ ions (α and β isomers of fully oxidized, one- and two-electron reduced ions). The kinetic data are plotted using the extended Debye–Hückel equation, in which the distance of closest contact is set equal to twice the hydrodynamic radius of a Keggin anion. In all cases, slopes of these plots give charge-product (z_1z_2) values within error of those anticipated based on the charges of the reacting ions. The aqueous solution chemistry of α-$AlW_{12}O_{40}^{5-}$ (α-$\mathbf{2}_{ox}$) and α-$AlW_{12}O_{40}^{6-}$ (α-$\mathbf{2}_{1e}$) is then fully defined, and the reduction potential of the α-$\mathbf{2}_{ox}$/α-$\mathbf{2}_{1e}$ couple is determined. These studies provide the information needed to use α-$\mathbf{2}_{1e}$, a powerful reducing agent, to obtain detailed information about the first steps in reduction of O_2 to H_2O, a process of considerable importance to chemistry and biology.

Keywords: Heteropolytungstate; Electron transfer; Water; Ionic-strength; Dioxygen

1. Introduction

Keggin heteropolytungstate cluster-anions [1] have been used in catalysis of O_2 oxidations [2], and as well-defined probes in kinetic studies of electron-transfer processes [3,4]. In 1983, Eberson [5] used $Co^{III}W_{12}O_{40}^{5-}$ to investigate the mechanism of electron-transfer oxidation of benzyllic C–H bonds. The data analysis included use of the Marcus cross relation [6], the application of which took advantage of kinetic parameters (reorganization energies, λ) published by Rasmussen and Brubaker [7] in 1964. These λ values were obtained by measuring the rates the electron self-exchange between $Co^{III}W_{12}O_{40}^{5-}$ and $Co^{II}W_{12}O_{40}^{6-}$. Since 1983, $Co^{III}W_{12}O_{40}^{5-}$, and the reduced anion, $Co^{II}W_{12}O_{40}^{7-}$ (an electron donor), as well as other Keggin anions, simpler isopolyanions, and Wells–Dawson anions, have been used as mechanistic probes to investigate a wide range of electron transfer reactions, involving both inorganic and organic substrates [3].

A general issue that arises in this chemistry is the need to determine the zero-ionic strength rate constants, k_{11}, for electron self exchange between oxidized and reduced forms of the heteropolytungstate cluster-anion probes. This fundamental parameter, a function of the reorganization energy, λ, describes the barrier to electron transfer to, or from, the cluster anion. In order to obtain k_{11} values associated with reactions of heteropolyanions, however, the ionic-strength dependence of the electron self-exchange reaction rates must be evaluated. This is an inevitable consequence of the large charges possessed by these cluster anions, and the large anion–anion repulsions (i.e., the large charge products, z_1z_2) involved in collisions between the reacting anions. It is critical that theoretical evaluation of the ionic-strength dependence of these reactions be handled properly. If this is done, reliable k_{11} values, and the inherent reorganization energies associated purely with changes in bond lengths and angles upon electron transfer (but not due to electrostatic interactions between reacting species) can be extracted from reaction rate data. Once a reliable k_{11} value has been determined for a specific pair of electron exchanging cluster anions, either partner in this reaction can be used to obtain fundamental information about a wide range of electron-transfer processes.

* Corresponding author.
E-mail address: iaw@sci.ccny.cuny.edu (I.A. Weinstock).

1381-1169/$ – see front matter © 2006 Elsevier B.V. All rights reserved.
doi:10.1016/j.molcata.2006.02.018

Moreover, the large charges of these clusters can then be used to advantage in studies of processes that involve the build-up of charge in substrate donors or acceptors during electron transfer itself.

In 1990, Kozik and Baker [8] used ^{31}P NMR to measure rates of electron self exchange between α-$PW_{12}O_{40}^{3-}$ ($\mathbf{1}_{ox}$) and the one-electron reduced ion, α-$PW_{12}O_{40}^{4-}$ ($\mathbf{1}_{1e}$), and between $\mathbf{1}_{1e}$ and the two-electron reduced ion, α-$PW_{12}O_{40}^{5-}$ ($\mathbf{1}_{2e}$). Despite the large charges of these reacting species, rates of electron self-exchange in water at low pH values varied with ionic strength according to the extended Debye–Hückel [9] equation:

$$\log k = \log k_0 + 2z_1z_2\alpha\mu^{1/2}/(1 + \beta r\mu^{1/2}) \quad (1)$$

In Eq. (1), $\alpha = 0.509$, $\beta = 0.33 \times 10^8$ cm (constants of the theory), and r is the hard-sphere collision distance. The collision distance, r, was set at 1.12 nm, twice the hydrodynamic radius of a Keggin ion in water [4,10]. For self-exchange between $\mathbf{1}_{ox}$ and $\mathbf{1}_{1e}$, a straight line was obtained (correlation coefficient = 0.998), whose slope gave a charge product, z_1z_2 of 14.1, close to the theoretical z_1z_2 value of 12. Similarly, for reaction between $\mathbf{1}_{1e}$ and $\mathbf{1}_{2e}$, the slope obtained from a plot of Eq. (1) gave a z_1z_2 value of 20, identical to the theoretical z_1z_2 value for reaction between the four- and five-minus ions.

We now show that, for self-exchange reactions between a series of $AlW_{12}O_{40}^{n-}$ ions (α and β isomers of fully oxidized, one- and two-electron reduced ions), plots of the extended Debye–Hückel equation give z_1z_2 values within error of those predicted by theory. Of these, the self-exchange reaction between α-$AlW_{12}O_{40}^{5-}$ ($\mathbf{2}_{ox}$) and α-$AlW_{12}O_{40}^{6-}$ ($\mathbf{2}_{1e}$) is investigated in detail. In addition, the reduction potential of the $\mathbf{2}_{ox}/\mathbf{2}_{1e}$ couple is determined, and the aqueous chemistry of both ions is defined. Issues addressed include stability in water over a range of pH values, and the extent of ion pairing with Keggin counter-cations, electrolyte cations, or with H^+ (at low pH values). Together, these studies provide the theoretical framework and physical data needed to use $\mathbf{2}_{1e}$ – a powerful reducing agent, that is stable and free of ion pairing over a wide range of pH values – to obtain detailed information about the first steps in reduction of O_2 to H_2O, a process of considerable importance to chemistry and biology.

2. Experimental

2.1. Synthesis

The sodium salt of $\mathbf{1}_{ox}$, α-$Na_3P^VW_{12}O_{40}{\cdot}xH_2O$, was purchased from Sigma–Aldrich Inc., while α- and β-$Na_5Al^{III}W_{12}O_{40}$ [11–13], were prepared using published methods. One- and two-electron reduced forms of the above ions were prepared in water (under argon) by constant-potential electrolysis.

2.2. Aqueous electrolyte solutions

Water for the preparation of solutions was obtained from a Barnstead Nanopure® water-purification system, and all chemicals and salts used in the preparation of buffers, or as electrolytes, were of the highest purity available from commercial sources. Ionic strength was varied by additions of NaCl, and reported ionic-strength values include contributions from the Keggin ion salts. pD values of D_2O solutions were calculated using $pD = pH_{el} + 0.4$, where pH_{el} values are readings from standard pH electrodes immersed in the D_2O solutions [14,15].

2.3. Instrumentation

UV–vis spectra were acquired using a Hewlett-Packard 8452A spectrophotometer equipped with a diode-array detector, a StellarNet Inc. EPP2000 spectrophotometer equipped with an immersible fiber-optic probe, a magnetic stirrer and a HP 89090A temperature controller. In some experiments, reaction rates were measured using an SF-61 stopped-flow instrument (Hi-Tech Scientific, UK). Al-27 NMR [11] spectra were acquired on a GE QE300 MHz spectrometer at 78.216 MHz, using a pulse width of 15 μs, and a sweep width of 12,500 Hz, and field homogeneity was tuned using D_2O for internal lock signals. Chemical-shift values are referenced to 0.1 M $AlCl_3$ in 1.0 M aqueous HCl ($[Al(H_2O)_6]^{3+}$, which was assigned a chemical shift of $\delta = 0$ ppm. This solution was used either as an external standard for integration of ^{27}Al NMR signals, or as an internal reference by placing the solution in the inner compartment of a coaxial NMR tube. Spectral data were processed using the NMR software package, NUTS (1-D version, Acorn NMR Inc., Fremont, CA).

2.4. Electrochemistry

Cyclic voltammograms were obtained at room temperature using a BAS CV-50 W electrochemical analyzer equipped with a glassy-carbon working electrode, a Pt-wire auxiliary electrode, and a Ag/AgCl (3 M NaCl) BAS reference electrode. Solutions analyzed were buffered, and contained 1–6 mM concentrations of Keggin ions, and total ionic strengths of from 0.05 to 1.20 M (NaCl). Scan rates were varied from 20 to 400 mV s^{-1}. The BAS reference electrode was calibrated using the $[Fe(CN)_6]^{3-}/[Fe(CN)_6]^{4-}$ couple, [16] at ionic strengths relevant to the present work (see below). Based on these data, reduction potentials, $E_{1/2}$ are reported relative to the normal hydrogen electrode (NHE) by addition of 250 mV to observed BAS electrode values.

Aqueous solutions of one- and two-electron reduced Keggin ions, α-$PW_{12}O_{40}^{4-}$ ($\mathbf{1}_{1e}$), α-$AlW_{12}O_{40}^{6-}$ (α-$\mathbf{2}_{1e}$), α-$AlW_{12}O_{40}^{7-}$ (α-$\mathbf{2}_{2e}$), β-$AlW_{12}O_{40}^{6-}$ (β-$\mathbf{2}_{1e}$), and β-$AlW_{12}O_{40}^{7-}$ (β-$\mathbf{2}_{2e}$), were prepared by bulk electrolysis under Ar using a reticulated vitreous-carbon working electrode. The auxiliary electrode, a coiled Pt-wire, was placed in a separate compartment, connected by fritted glass. The reactions were carried out using 0.1 M buffer solutions. For determination of electron-self exchange rate constants by ^{27}Al NMR spectroscopy, 1:1 mixtures of D_2O and water were used. Samples for NMR spectroscopy were transferred to Ar-filled NMR tubes, using standard Schlenk techniques. Once flame sealed, these tubes were kept for several months without noticeable changes in NMR spectra. Extinction coefficients of reduced Keg-

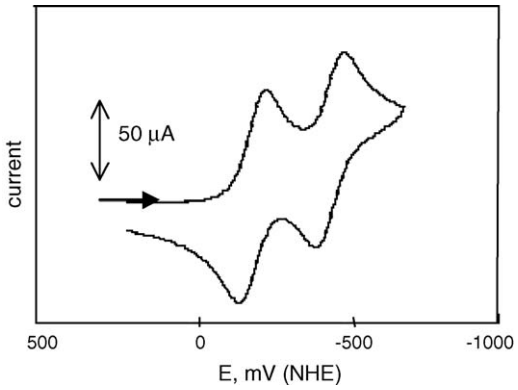

Fig. 1. Cyclic voltammogram of α-$AlW_{12}O_{40}^{5-}$ (α-**2**) in 50 mM phosphate (pH 7.2) and 0.1 M NaCl; sweep rate = 100 mV/s. Currents shown are associated with the first and second one-electron reductions.

gin (POM) anions were determined by UV–vis spectroscopy after bulk electrolysis of solutions containing a range of Keggin ion concentrations.

2.5. Reaction rates

Electron self-exchange rate constants were obtained by analysis of line broadening in ^{27}Al NMR spectra of mixtures of fully oxidized, one-, and two-electron reduced, α- and β-Keggin dodecatungstoaluminates, as a function of ionic strength, and at several pH values. Independent verification of the zero-ionic strength ($\mu = 0$ M) self-exchange rate constant, k_{11}, determined for self-exchange between α-$\mathbf{2}_{ox}$ and α-$\mathbf{2}_{1e}$, was provided by the cross-reaction: α-$\mathbf{2}_{1e}$ + α-$PW_{12}O_{40}^{4-}$ ($\mathbf{1}_{1e}$) → α-$\mathbf{2}_{ox}$ + $\mathbf{1}_{2e}$ ($2e^-$ reduced).

3. Results and discussion

3.1. Solution chemistry of α and β-$AlW_{12}O_{40}^{5-}$

At pH 7.2 in phosphate buffer, the first and second one-electron couples of α- and β-$AlW_{12}O_{40}^{5-}$ are electrochemically reversible. A representative cyclic voltammegram is provided in Fig. 1, and data for both isomers are summarized in Table 1.

Additional solution studies [17] further established that, at room temperature in pH-buffered aqueous solutions, pure α-$\mathbf{2}_{1e}$ is stable with respect to three plausible processes: (1) isomerization to the β-Keggin structure [11,12,18], (2) disproportionation to mixtures of α-$\mathbf{2}_{ox}$, α-$\mathbf{2}_{1e}$, and the two-electron-reduced anion α-$AlW_{12}O_{40}^{7-}$, and (3) acid-decomposition at low pH values, or hydrolysis at neutral pH values, to give defect "lacunary" species with less than a full complement of 12 W "addendum" atoms [11–13].

Table 1
First and second one-electron reduction potentials of α- and β-$AlW_{12}O_{40}^{5-}$ relative to the normal hydrogen electrode (NHE)[a]

Isomer	$n^-/(n+1)^-$	pH range	E (mV)
α	$5^-/6^-$	1.8–7.5	−130
α	$6^-/7^-$	2.05	−330
α	$6^-/7^-$	3.00	−350
α	$6^-/7^-$	7.2	−360
β	$5^-/6^-$	7.2	−45
β	$6^-/7^-$	7.2	−310

[a] Data obtained in 0.05 M buffer solutions, 0.15 M in NaCl.

Keggin undecatungstoaluminates (α and β isomers of $AlW_{12}O_{40}^{5-}$, $AlW_{12}O_{40}^{6-}$ and $AlW_{12}O_{40}^{7-}$) are stable to hydrolysis at room temperature over a wide range of pH values (from less than 0 to larger than 7). This was confirmed quantitatively by cyclic voltammetry and ^{27}Al NMR spectroscopy. First, cyclic voltammograms (CVs; peak currents, peak separations, and reduction potentials) remained unchanged throughout repeated cycles of electrochemical reduction/re-oxidation, and before and after bulk electrolytic reduction at pH 7.2, in phosphate buffer (Table 2). CVs also remained unchanged when electrochemically reduced solutions of **2** were re-oxidized by exposure to dioxygen (O_2 in ambient air); no differences were observed between these solutions and those subjected to electrochemical reduction/re-oxidation cycles. So, too, the ^{27}Al NMR spectra of all these solutions (number, location, intensities and line-widths of the ^{27}Al NMR signals) also remained unchanged (Table 2). These data show that the reduction and chemical- or electrochemical-oxidation processes are all reversible, neither altering Keggin-ion concentrations, nor resulting in detectable quantities of isomerization, disproportionation or hydrolysis products.

In additional control experiments, equilibrated solutions of mixtures of α-$\mathbf{2}_{ox}$ and α-$\mathbf{2}_{1e}$, and of mixtures of α-$\mathbf{2}_{1e}$ and the two-electron-reduced anion, α-$\mathbf{2}_{2e}$, were stored under argon at room temperature in flame-sealed NMR tubes. After 6 months, no changes were observed by ^{27}Al NMR spectroscopy. No β isomers or decomposition products were observed, and ratios of oxidized to reduced anions remained unchanged, an indication that disproportionation of α-$\mathbf{2}_{1e}$ to give α-$\mathbf{2}_{2e}$ and α-$\mathbf{2}_{ox}$ had not occurred.

Disproportionation of α-$\mathbf{2}_{1e}$ was further ruled out by mixing α-$\mathbf{2}_{2e}$ with an excess of α-$\mathbf{2}_{ox}$ at pH 7.2 in phosphate buffer. The reaction, followed by UV–vis spectroscopy at 480 nm, proceeded to completion [17], giving two equivalents of α-$\mathbf{2}_{1e}$ (no α-$\mathbf{2}_{2e}$ was observed).

3.2. ^{27}Al NMR spectra

The overall T_d symmetry of α-$\mathbf{2}_{ox}$ reflects the nearly ideal T_d geometry about the four-coordinate Al(III) ion at its center [11]. As a result of this high overall (cluster) and local ($Al^{III}O_4^{5-}$ oxoanion) symmetry, the ^{27}Al NMR spectrum of α-$\mathbf{2}_{ox}$ contains a single, narrow signal ($\nu_{1/2} = 0.77 \pm 0.05$ Hz; Fig. 2B) [11]. Although crystallographic data [19] show the central $Al^{III}O_4^{5-}$ fragment in β-$AlW_{12}O_{40}^{5-}$ (β-$\mathbf{2}_{ox}$) to be a nearly ideal tetrahedron, the symmetry of the $W_{12}O_{36}$ shell has decreased from T_d (for α) to C_{3v} (for β). This results in a five-fold increase in line-width of the ^{27}Al NMR signal of from 0.77 ± 0.05 Hz for α-$AlW_{12}O_{40}^{5-}$ (α-$\mathbf{2}_{ox}$), to 3.9 Hz for β-$AlW_{12}O_{40}^{5-}$ (β-$\mathbf{2}_{ox}$).

By contrast, the line-widths of the ^{27}Al NMR signals in α-$\mathbf{2}_{ox}$ and α-$\mathbf{2}_{1e}$ are statistically identical. This shows that little if any structural change occurs upon reduction of α-$\mathbf{2}_{ox}$ and α-$\mathbf{2}_{1e}$. This

Table 2
First and second cathodic and anodic potentials[a] (E_a and E_c), peak currents (I_a and I_c) and ^{27}Al NMR signal intensities[b] of α-and β-$Na_5AlW_{12}O_{40}$ before and after cycles of electrochemical reduction, and electrochemical or O_2 re-oxidation[c]

Entry	Reaction sequences	E_a (mV)	E_c (mV)	I_a ($\times 10^5$ A)	I_c ($\times 10^5$ A)	^{27}Al NMR ratio: $[\mathbf{2}_{ox}]/[Al(H_2O)_6^{3+}]$
1	Fully oxidized α-$AlW_{12}O_{40}^{5-}$ (α-$\mathbf{2}_{ox}$)	−170	−90	4.7	3.2	2.7 ± 0.1
		−420	−340	3.5	4.0	
2	2e-reduction to α-$AlW_{12}O_{40}^{7-}$ (α-$\mathbf{2}_{2e}$) at −900 mV					
3	Electrochemical re-oxidation to α-$\mathbf{2}_{ox}$ at −50 mV	−173	−101	4.8	3.8	2.7 ± 0.1
		−425	−351	3.6	4.3	
4	2e-reduction to α-$\mathbf{2}_{2e}$ at −780 mV					
5	O_2 re-oxidation to α-$\mathbf{2}_{ox}$	−178	−100	4.7	3.4	2.8 ± 0.1
		−427	−351	3.45	3.9	
6	Fully oxidized β-$AlW_{12}O_{40}^{5-}$ (β-$\mathbf{2}_{ox}$)	−82	−9	4.85	3.8	2.0 ± 0.1
		−347	−269	3.8	4.7	
7	2e-reduction to β-$AlW_{12}O_{40}^{7-}$ (β-$\mathbf{2}_{2e}$) at −780 mV					
8	Electrochemical re-oxidation to β-$\mathbf{2}_{ox}$ at −50 mV	−79	−9	4.9	3.9	See entry 10
		−350	−268	3.8	4.7	
9	2e-reduction to β-$\mathbf{2}_{2e}$ at −780 mV					
10	O_2 re-oxidation to β-$\mathbf{2}_{ox}$	−80	−6	4.8	4.0	2.0 ± 0.1
		−350	−268	4.0	5.0	

[a] Relative to NHE.
[b] Relative to $Al(H_2O)_6^{3+}$.
[c] [**2**] = 4.6 mM, 50 mM phosphate buffer and 0.17 M NaCl; pH/pD = 7.2, D_2O:H_2O = 1:1. All measurements were obtained at ambient temperature.

holds true for alpha anions. As shown in Table 3, however, ^{27}Al line-widths in ^{27}Al NMR spectra of β isomers increase from 3.9 to 4.25 Hz for the fully oxidized and one-electron reduced anions, β-$AlW_{12}O_{40}^{5-}$ (β-$\mathbf{2}_{ox}$) and β-$AlW_{12}O_{40}^{6-}$ (β-$\mathbf{2}_{1e}$), to 25 ± 5 Hz for the two-electron-reduced β anion, β-$AlW_{12}O_{40}^{7-}$ (β-$\mathbf{2}_{2e}$). While beyond the scope of the present work, this trend suggests that sensitivity of the quadrupolar (I = 5/2) ^{27}Al nucleus to subtle changes in anion symmetry might provide insight into the electronic structure of two-electron-reduced Keggin anions.

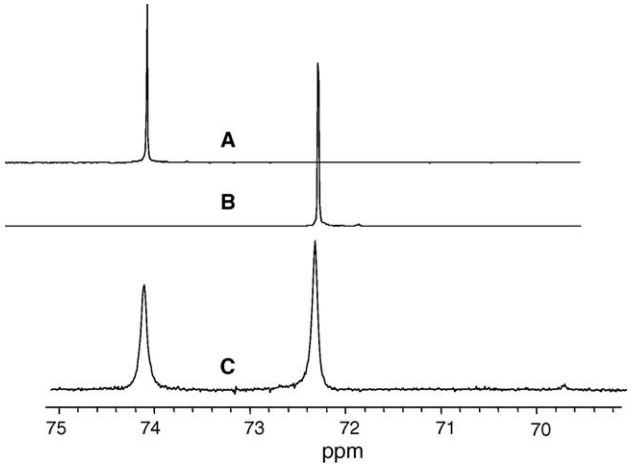

Fig. 2. ^{27}Al NMR spectra of α-$AlW_{12}O_{40}^{6-}$ (α-$\mathbf{2}_{1e}$) (A), α-$AlW_{12}O_{40}^{5-}$ (α-$\mathbf{2}_{ox}$) (B), and a mixture containing a 1.0–0.85 molar ratio of α-$\mathbf{2}_{ox}$ to α-$\mathbf{2}_{1e}$ (C). The total concentration of Keggin anions present (both α-$\mathbf{2}_{ox}$ and α-$\mathbf{2}_{1e}$) was 4.6 mM; [NaCl] was 0.68 M, at pH 7.2 and 19.2 ± 0.5 °C.

3.3. Electron self-exchange reactions

As in self-exchange between $\mathbf{1}_{1e}$ and $\mathbf{1}_{ox}$ [8,20], electron transfer between α-$\mathbf{2}_{1e}$ and α-$\mathbf{2}_{ox}$ obeys the following rate expression [17]:

$$\text{rate} = k[\alpha\text{-}\mathbf{2}_{1e}][\alpha\text{-}\mathbf{2}_{ox}], \quad (2)$$

where k is the bimolecular rate constant. The line width, $\Delta\nu_{red}$, of the ^{27}Al NMR signal of α-$\mathbf{2}_{1e}$, at equilibrium in solution with α-$\mathbf{2}_{ox}$, is given by:

$$\Delta\nu_{1e} = 1/(\pi T_{mixture}) = 1/(\pi T_2) + 1/(\pi\tau), \quad (3)$$

where $T_{mixture}$ is the total relaxation time associated with α-$\mathbf{2}_{1e}$ at equilibrium in solution with α-$\mathbf{2}_{ox}$, T_2 the relaxation time of pure α-$\mathbf{2}_{1e}$, τ the life-time of α-$\mathbf{2}_{1e}$ in its reaction with α-$\mathbf{2}_{ox}$,

Table 3
Chemical shifts (ppm) and line-widths (Hz) of Al(III)-heteroatom signals in ^{27}Al NMR spectra of fully oxidized, and one- and two-electron reduced α- and β-dodecatungstoaluminates

Entry	Anion	Chemical shift[a] (ppm)	Line-width (Hz)
1	α-$AlW_{12}O_{40}^{5-}$ (α-$\mathbf{2}_{ox}$)	72.3	0.77 ± 0.05
2	α-$AlW_{12}O_{40}^{6-}$ (α-$\mathbf{2}_{1e}$)	74.1	0.76 ± 0.05
3	α-$AlW_{12}O_{40}^{7-}$ (α-$\mathbf{2}_{2e}$)	68.9	1.5 ± 0.1
4	β-$AlW_{12}O_{40}^{5-}$ (β-2$_{ox}$)	71.9	3.9 ± 0.2
5	β-$AlW_{12}O_{40}^{6-}$ (β-2$_{1e}$)	69.7	4.25 ± 0.2
6	β-$AlW_{12}O_{40}^{7-}$ (β-2$_{2e}$)	68.3	25 ± 8

[a] Relative to $Al(H_2O)_6^{3+}$ (in 1 M HCl (aq.)). Conditions: 19.2 ± 0.5 °C; pH/pD = 7.2 (H_2O:D_2O = 1:1).

$1/(\pi T_2)$ the line width of pure α-$\mathbf{2}_{1e}$ ($\Delta\nu_{1e}{}^0$), and $\tau = 1/(k[\alpha\text{-}\mathbf{2}_{ox}])$. Substitution and rearrangement give:

$$k = (\Delta\nu_{1e} - \Delta\nu_{1e}{}^0)\pi/[\alpha\text{-}\mathbf{2}_{ox}] \quad (4)$$

Similarly, k, as a function of broadening in the ^{27}Al NMR signal of α-$\mathbf{2}_{ox}$, at equilibrium with α-$\mathbf{2}_{1e}$, is given by:

$$k = (\Delta\nu_{ox} - \Delta\nu_{ox}{}^0)\pi/[\alpha\text{-}\mathbf{2}_{1e}], \quad (5)$$

where $\Delta\nu_{ox}{}^0$ is the line width of pure α-$\mathbf{2}_{ox}$.

Rate constants, k (rate $= k[\alpha\text{-}\mathbf{2}_{ox}][\alpha\text{-}\mathbf{2}_{1e}]$) were obtained from measurements of ^{27}Al NMR spectra as ionic strength, μ, was varied (addition of NaCl) at the slow-exchange limit. A representative set of ^{27}Al NMR spectra is shown in Fig. 2.

The functional dependence of $\log k$ on μ was calculated using the extended Debye–Hückel equation [9]: $\log k = \log k_0 + 2\alpha z_1 z_2 \mu^{1/2}/(1 + \beta r \mu^{1/2})$, ($\alpha = 0.509$, $\beta = 0.33 \times 10^8$ cm, z_1 and z_2 are the charges of the reacting anions, and r is the hard-sphere collision distance, 1.12 nm). Plots of the extended Debye–Hückel equation, based on data obtained from line broadening in ^{27}Al NMR spectra (and from analogs of Eqs. (4) and (5)), were obtained for electron self-exchange reactions between: α-$AlW_{12}O_{40}{}^{6-}$ and α-$AlW_{12}O_{40}{}^{5-}$, α-$AlW_{12}O_{40}{}^{7-}$ and α-$AlW_{12}O_{40}{}^{6-}$, and between β-$AlW_{12}O_{40}{}^{6-}$ and β-$AlW_{12}O_{40}{}^{5-}$, and β-$AlW_{12}O_{40}{}^{7-}$ and β-$AlW_{12}O_{40}{}^{6-}$ (Figs. 3 and 4). In all cases, plots of the extended Debye–Hückel equation give charge products within experimental uncertainty of theoretical values.

For self-exchange between α-$AlW_{12}O_{40}{}^{6-}$ (α-$\mathbf{2}_{1e}$) and α-$AlW_{12}O_{40}{}^{5-}$ (α-$\mathbf{2}_{ox}$), the reaction studied in the greatest detail, ionic strength, μ, was varied from 0.18 to 1.1 M. Plot of $\log k$ as a function of μ, using the extended Debye–Hückel equation (Fig. 3 (bottom)), gives a line ($R^2 = 0.996$), whose slope gives the charge product, $z_1 z_2$, and whose y-intercept gives k_{11} at $\mu = 0$ (the self-exchange rate constant at zero ionic strength).

Close agreement of the calculated charge product (from the slope of the lower-most plot in Fig. 3) with the theoretical value, $z_1 z_2 = 30$ (where z_1 and z_2 are 6^- and 5^-, the charges of α-2_{1e} and α-2_{ox}), shows compliance with the extended Debye–Hückel equation, a prerequisite to the defensible application of theoretical models, such as those of Marcus and Sutin, to outer-sphere electron-transfer reactions between charged donors and acceptors. The parameters α and β used in the extended Debye–Hückel equation, are standard values for ions in water at 25 °C. The charge product of 29 ± 2 thus indicates that: (1) α-2_{1e} and α-2_{ox} behave in aqueous NaCl as charged, 6^- and 5^-, spheres, each with of radius 5.6 Å [11], (2) ion pairing with Na^+ is negligible at NaCl concentrations as large as 1.1 M, and (3) that cation (Na^+) catalysis [21] of electron exchange between the two ions, is not kinetically significant.

In addition, the rate of self-exchange varied with μ, but not with pH (c.f. the solid diamond in Fig. 3 (lowermost plot)). In a control experiment pertinent to variation of [α-$\mathbf{2}_{1e}$] in kinetic studies of electron donation by α-$\mathbf{2}_{1e}$, two rate constants (open circles) were obtained after doubling total Keggin ion concentrations to 9.2 mM. Finally, extrapolation to zero ionic strength ($\mu = 0$), gave $k_{11} = (6.5 \pm 1.5) \times 10^{-3}\ M^{-1}\ s^{-1}$.

Plots for the other three self-exchange reactions (Figs. 3 and 4), were similarly calculated by setting the hard-sphere collision distance, r equal to 1.12 nm. The experimental uncertainties, and scatter in the data, are somewhat larger for reactions of the two-electron reduced ions, and β isomers. This is likely due to the larger line-widths associated with these ions (see Table 3 (above)), in relation to which, small increases in line widths at the slow-exchange limit on the ^{27}Al NMR timescale were less pronounced, and smaller relative to experimental uncertainties.

Charge products, $z_1 z_2$, and zero-ionic-strength rate constants, k_{11}, for all four self-exchanging pairs are listed in Table 4. In all cases, slopes of the plots in Figs. 3 and 4 give charge products close to theoretical (actual ion-charge) values.

3.4. Ionic-strength dependence of self-exchange rate constants

In the data provided here, the functional dependence of bimolecular rate constants on ionic strength is accurately

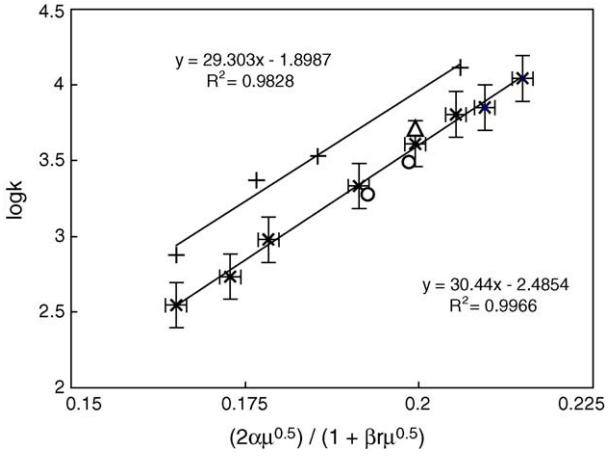

Fig. 3. Plot of $\log k$ vs. $(2\alpha\mu)^{0.5}/(1 + \beta r\mu^{0.5})$ for electron-exchange reactions between α-$AlW_{12}O_{40}{}^{5-}$ and α-$AlW_{12}O_{40}{}^{6-}$ ((✱), (△), and (◯)) and between β-$AlW_{12}O_{40}{}^{5-}$ and β-$AlW_{12}O_{40}{}^{6-}$ (+). $[POM]_{total} = 4.6$ mM ((+), (△), and (✱)) and 9.2 mM (◯); pH/pD 7.2 (2.15 for (△)); D_2O:H_2O = 1:1; 19.2 ± 0.5 °C. Uncertainties (shown as error bars here) and in k_{11} and in $z_1 z_2$ (reported in the text and in Table 4) are 95% confidence intervals.

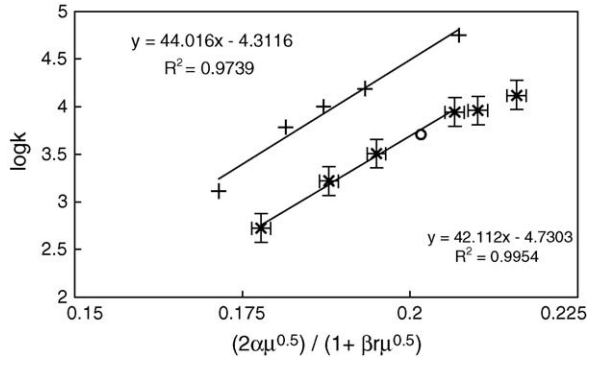

Fig. 4. Plot of $\log k$ vs. $(2\alpha\mu)^{0.5}/(1 + \beta r\mu^{0.5})$ for electron-exchange reactions between α-$AlW_{12}O_{40}{}^{6-}$ and α-$AlW_{12}O_{40}{}^{7-}$ ((✱) and (◯)) and between β-$AlW_{12}O_{40}{}^{6-}$ and β-$AlW_{12}O_{40}{}^{7-}$ (+). $[POM]_{total} = 4.6$ mM (✱) and 9.2 mM (◯); pH/pD 7.2; D_2O:H_2O = 1:1; 19.2 ± 0.5 °C. As in Fig. 3, the error bars on data points (✱) are 95% confidence intervals.

Table 4
Charge products and zero-ionic strength rate constants from plots in Figs. 3 and 4

Reacting anions	$\log k_{11}$	k_{11} ($M^{-1}\,s^{-1}$)	z_1z_2[a] (experimental)	z_1z_2[b] (theoretical)
α-$AlW_{12}O_{40}^{5-}$/α-$AlW_{12}O_{40}^{6-}$	-2.2 ± 0.15	6×10^{-3}	30 ± 2	30
α-$AlW_{12}O_{40}^{6-}$/α-$AlW_{12}O_{40}^{7-}$	-4.7 ± 0.4	2×10^{-5}	41 ± 3	42
β-$AlW_{12}O_{40}^{5-}$/β-$AlW_{12}O_{40}^{6-}$	-1.9 ± 0.5	1×10^{-2}	29 ± 3	29
β-$AlW_{12}O_{40}^{6-}$/β-$AlW_{12}O_{40}^{7-}$	-4.3 ± 0.8	5×10^{-5}	43 ± 4	42

[a] Values of the charge products z_1z_2 are from the slopes of the plots in Figs. 3 and 4. In each case, the charge products are within error of theoretically predicted values.
[b] Values are the products of the charges of the reacting cluster anions. Experimental uncertainties were calculated using "Data Analysis ToolPak: Regression," from MS Excel software.

accounted for by the extended Debye–Hückel equation. This is by no means a general result for all Keggin ions under all conditions. For example, in electron transfer between α-$AlW_{12}O_{40}^{6-}$ (α-$\mathbf{2}_{1e}$) and $Cu^{II}W_{12}O_{40}^{6-}$, catalysis by Na^+ is observed. In these and other cases in which electron transfer is catalyzed by cations present in solution, the Debye–Hückel equation either fails to provide a linear correlation between reaction rates, k, and ionic strength, or, if linear plots are obtained, the charge products, z_1z_2 obtained from their slopes, are quite different from theoretically predicted values. In cases where cation catalysis is either not kinetically significant, or is deliberately suppressed by the addition of chelating agents, experimental and theoretical z_1z_2 consistently agree with one another.

An additional (practical) test for applicability of the extended Debye–Hückel equation is whether the zero-ionic strength rate constants, k_{11}, provide experimentally verifiable values when used in the Marcus cross relation. To evaluate this, α-$\mathbf{2}_{1e}$ was reacted with α-$PW_{12}O_{40}^{4-}$ ($\mathbf{1}_{1e}$) (Eq. (6)), and reaction rates measured using a stopped-flow apparatus.

$$\alpha\text{-}\mathbf{2}_{1e} + \alpha\text{-}PW_{12}O_{40}^{4-}(\mathbf{1}_{1e}) \rightarrow \alpha\text{-}\mathbf{2}_{ox} + \alpha\text{-}PW_{12}O_{40}^{5-} \quad (\mathbf{1}_{2e};\ 2e^-\ \text{reduced}) \tag{6}$$

This reaction was chosen because experimental rate constants (determined by ^{31}P NMR), have been reported for the relevant electron self-exchange reaction: α-$PW_{12}O_{40}^{5-}$ + α-$PW_{12}O_{40}^{4-}$ [8]. Bimolecular rate constants (at three experimentally accessible ionic-strength values) were plotted as a function of ionic strength using the extended Debye–Hückel equation. The slope gave a charge product (z_1z_2; product of the charges of α-$\mathbf{2}_{1e}$ and $\mathbf{1}_{1e}$) of 23 ± 1, within experimental uncertainty of the theoretical values of 24. Extrapolation to zero ionic strength gave $k_{12} = 17 \pm 2\,M^{-1}\,s^{-1}$. The rate constant for self-exchange between α-$\mathbf{2}_{1e}$ and α-$\mathbf{2}_{ox}$ ($(6.5 \pm 1.5) \times 10^{-3}\,M^{-1}\,s^{-1}$), was then used in the Marcus cross relation to estimate $k_{0(calc)}$ for electron transfer from α-$\mathbf{2}_{1e}$ to $\mathbf{1}_{1e}$ at zero ionic strength. Also used in this calculation were the published [8] rate constant for self-exchange between $\mathbf{1}_{1e}$ and α-$PW_{12}O_{40}^{5-}$ ($(1.6 \pm 0.3) \times 10^2\,M^{-1}\,s^{-1}$), and the reduction potentials, -130 ± 5 and -10 ± 5 mV, respectively, for the self-exchanging couples, α-$\mathbf{2}_{1e}$/α-$\mathbf{2}_{ox}$ and $\mathbf{1}_{1e}$/α-$PW_{12}O_{40}^{5-}$. All work-term corrections [22], though small, were included. The Marcus cross relation gave $k_{0(calc)} = 13 \pm 6\,M^{-1}\,s^{-1}$. This value, within experimental uncertainty of that obtained by stopped-flow measurements ($17 \pm 2\,M^{-1}\,s^{-1}$), provides an independent and practically relevant support for use of the extended Debye–Hückel equation. This also argues that agreement between experimental and theoretical charge products (as was observed for both of the self-exchange reactions involved in the cross reaction described here), is a valid criterion for applicability of the extended Debye–Hückel model to electron-transfer reactions of Keggin ions.

It must be noted, however, that solutions of *mixed* electrolytes, such as those almost always encountered in kinetic studies in water, do not *rigorously* satisfy the thermodynamic criteria for which the extended Debye–Hückel equation was derived [9]. At the same time, other models, such as the full Guggenheim equation [9], while rigorously correct thermodynamically, were not derived for highly charged ions, and like even the *extended* Debye–Hückel equation itself, are strictly applicable only to solutions whose ionic strengths do not exceed 0.1 M. Attempts to model our data using the Debye–Hückel or Guggenheim equations gave incorrect charge products (i.e., theoretical values were off by more than 50%). Notably, the Guggenheim equation eliminates explicit use of r, the distance of closest approach of the reacting ions, and, instead introduces interaction coefficients, B, as empirical corrections to the Debye–Hückel equation. The extended Debye–Hückel equation, on the other hand, *explicitly includes the distance of closest approach*, r, *of the colliding ions*. In light of agreement between theory and experiment in Figs. 3 and 4, where r was set at twice the crystallographic radius of a Keggin anion, it appears that explicit inclusion of the distance of closest approach is critically important, and practically useful, for evaluating reactions of Keggin ions in water.

3.5. Electron transfer reactions of Keggin heteropolytungstates

The above results raise a general question regarding the nature of Keggin heteropolytungstate ions in water. Kozik and Baker commented on this in 1990. For the self-exchange reaction between α-$PW_{12}O_{40}^{4-}$ and α-$PW_{12}O_{40}^{3-}$, they successfully used the extended Debye–Hückel equation to evaluate six rate constants, k, obtained at μ values that ranged from 0.26 to

0.616 M. All 6 k values lay on a straight line (correlation coefficient = 0.998), whose slope gave a charge product, z_1z_2 of 14.1, relatively close to the theoretical z_1z_2 value of 12. Kozik and Baker noted that, although the extended Debye–Hückel equation was originally derived only for ionic concentrations smaller than 0.01 M, it accounted for the ionic strength dependence of the rate constant at unexpectedly high ionic strengths of greater than 0.5 M. They suggested this was a consequence of the "fact that heteropoly anions, owing to the very pronounced inward polarization of their exterior oxygen atoms, have extremely low solvation energies and very low van der Waals attractions for one another". This is consistent with our observation that very little ion pairing between α-$\mathbf{2}_{1e}$ and Na^+ or H^+ occurs over wide ranges of concentrations of these cations. An additional factor is that Keggin-anion charges, distributed over many atoms, are highly diffuse, more so than for anions typically thought to be "non-coordinating". For example, while the single charge of perchlorate (ClO_4^-) is distributed over five atoms (a charge/atom ratio of 1/5, or 0.2), the 6^- charge of α-$\mathbf{2}_{1e}$ is distributed over 53 atoms (a ratio of 0.11). The diffuse nature of Keggin-ion charge stands in even greater contrast when compared with the ions in simple salts, such as NaCl, for which the extended Debye–Hückel equation was derived.

This analysis of the nature of Keggin heteropolytungstates in water is supported by the results of diffusion-rate [10,23], and density [24] measurements, which, through application of the Stokes–Einstein equation [25], argue that the effective hydrodynamic radii of 3-, 4-, 5- and 6-Keggin anions are *equal to* their crystallographic radii. This means that, on average, these Keggin anions are each solvated by no greater than one water molecule. This result again stands in sharp contrast to the aqueous solutions of alkali-metal cations such as Li^+ and Na^+, whose hydrodynamic radii of 3.40 and 2.76 Å suggest close association of each ion, respectively, with 25 and 17 water molecules [26].

These observations perhaps explain why use of the crystallographic radius of the Keggin ion (5.6 Å) as the basis for estimating the distance of closest contact in the extended Debye–Hückel equation (i.e., r = 11.2 Å), give plots whose slopes are so consistently close to theoretical z_1z_2 values, and zero-ionic strength rate constants that provide good agreement between experimentally determined rate constants (c.f. Eq. (6)), and values calculated using the Marcus cross relation.

4. Conclusions

The studies summarized here define the aqueous solution chemistry of α-$\mathbf{2}_{1e}$, and provide the *thermodynamic* values (reduction potential, $E_{1/2}$), and *kinetic* parameters (zero-ionic strength, self-exchange rate constant, k_{11}), needed to use α-$\mathbf{2}_{1e}$ as a mechanistic probe of electron transfer reactions in water. Ongoing and future mechanistic studies using α-$\mathbf{2}_{1e}$, include electron transfer to small molecules such as O_2, H_2, or NO, to biomimetic metallo-organic complexes, and redox-active enzymes, and the use of α-$\mathbf{2}_{1e}$ to provide fundamental information regarding relationships between cation motion (Na^+ and others) and charge transfer, in controlled reductions of metal, metal oxide or semiconductor quantum dots [27].

In the first of these studies, an *iso*-structural series of $1e^-$-reduced, α-Keggin heteropolytungstate cluster–anions (POM_{red}: α-$X^{n+}W_{12}O_{40}^{(9-n)-}$, where $X^{n+} = Al^{III}$, Si^{IV}, P^{V}), whose charges vary with X^{n+} from 6^- to 5^- to 4^-, and whose $1e^-$ reduction potentials, $E_{1/2}$, vary, respectively, from −0.130 to +0.055 to +0.255 V (NHE), are used to define the roles of both H^+ (variable-pH studies using α-$\mathbf{2}_{1e}$; $X^{n+} = Al^{3+}$), and Keggin-anion charge (use of all three donor anions at pH 2), in outer-sphere electron transfer to O_2 in water: $POM_{red} + O_2 + H^+ \rightarrow POM_{ox} + HO_2^{\bullet}$. These studies, to be reported separately, serve as an independent line of evidence in support of the k_{11} values obtained using the extended Debye–Hückel equation (work described above). Moreover, they provide a picture, unprecedented in its detail, of the physical properties (effective sizes, contact distances, and rates and energies of formation), of short-lived successor-complex ion pairs: $[(\alpha\text{-}X^{n+}W_{12}O_{40}^{(8-n)-})(O_2^-)]^{(9-n)-}$.

Acknowledgements

We thank the U.S. Department of Energy (DE-FC36-95GO10090), the U.S. Department of Agriculture (FS-FPL-4709), and PSC CUNY (60088-35-36) for support.

References

[1] M.T. Pope, in: A.G. Wedd (Ed.), In Comprehensive Coordination Chemistry II: From Biology to Nanotechnology, vol. 4, Elsevier Ltd., Oxford, UK, 2004, p. 635.
[2] C.L. Hill, in: A.G. Wedd (Ed.), In Comprehensive Coordination Chemistry II: From Biology to Nanotechnology, vol. 4, Elsevier Ltd., Oxford, UK, 2004, p. 679.
[3] I.A. Weinstock, Chem. Rev. 98 (1998) 113.
[4] V.A. Grigoriev, D. Cheng, C.L. Hill, I.A. Weinstock, J. Am. Chem. Soc. 123 (2001) 5292.
[5] L.J. Eberson, J. Am. Chem. Soc. 105 (1983) 3192.
[6] R.A. Marcus, Angew. Chem., Int. Ed. 32 (1993) 1111.
[7] P.G. Rasmussen, C.L. Brubaker Jr., Inorg. Chem. 3 (1964) 977.
[8] M. Kozik, L.C.W. Baker, J. Am. Chem. Soc. 112 (1990) 7604.
[9] A.D. Pethybridge, J.E. Prue, in: J.O. Edwards (Ed.), In Inorganic Reaction Mechanisms. Part II, vol. 17, Wiley, New York, 1972, p. 327.
[10] V.A. Grigoriev, C.L. Hill, I.A. Weinstock, J. Am. Chem. Soc. 122 (2000) 3544.
[11] I.A. Weinstock, J.J. Cowan, E.M.G. Barbuzzi, H. Zeng, C.L. Hill, J. Am. Chem. Soc. 122 (1999) 4608.
[12] J.J. Cowan, A.J. Bailey, R.A. Heintz, B.T. Do, K.I. Hardcastle, C.L. Hill, I.A. Weinstock, Inorg. Chem. 40 (2001) 6666.
[13] J.J. Cowan, C.L. Hill, R.S. Reiner, I.A. Weinstock, in: D. Coucouvanis (Ed.), Inorganic Synthesis, vol.33, Wiley, New York, 2002, p. 18.
[14] C.C. Westcott, pH Measurements, Academic Press, New York, 1978.
[15] G.-S. Kim, H. Zeng, W.A. Neiwert, J.J. Cowan, D. VanDerveer, C.L. Hill, I.A. Weinstock, Inorg. Chem. 42 (2003) 5537.
[16] R.E. Panzer, P.J. Elving, J. Electrochem. Soc. 119 (1972) 864.
[17] Y.V. Geletii, C.L. Hill, A.J. Bailey, K.I. Hardcastle, R.H. Atalla, I.A. Weinstock, Inorg. Chem. 44 (2005) 8955.
[18] X. Lopez, J.M. Maestre, C. Bo, J.-M. Poblet, J. Am. Chem. Soc. 123 (2001) 9571.
[19] W.A. Neiwert, J.J. Cowan, K.I. Hardcastle, C.L. Hill, I.A. Weinstock, Inorg. Chem. 41 (2002) 6950.

[20] M. Kozik, C.F. Hammer, L.C.W. Baker, J. Am. Chem. Soc. 108 (1986) 7627.
[21] P.D. Metelski, T.W. Swaddle, Inorg. Chem. 38 (1999) 301.
[22] R.A. Marcus, N. Sutin, Biochim. Biophys. Acta 811 (1985) 265.
[23] M.C. Baker, P.A. Lyons, S.J. Singer, J. Am. Chem. Soc. 77 (1955) 2011.
[24] T. Kurucsev, A.M. Sargeson, B.O. West, J. Phys. Chem. 61 (1957) 1567.
[25] J.T. Edward, J. Chem. Ed. 47 (1970) 261.
[26] F.A. Cotton, G. Wilkinson, Advanced Inorganic Chemistry, 4th ed., Wiley, New York, 1980.
[27] D.M. Adams, L. Brus, C.E.D. Chidsey, S. Creager, C. Creutz, C.R. Kagan, P.V. Kamat, M. Lieberman, S. Lindsay, R.A. Marcus, R.M. Metzger, M.E. Michel-Beyerle, J.R. Miller, M.D. Newton, D.R. Rolison, O. Sankey, K.S. Schanze, J. Yardley, X. Zhu, J. Phys. Chem. B 107 (2003) 6668.